Formation of smectic and columnar liquid crystalline phases by cyclotriveratrylene (CTV) and cyclotetraveratrylene (CTTV) derivatives incorporating calamitic structural units

Ralph Lunkwitz,[a] Carsten Tschierske*[a] and Siegmar Diele[b]

[a]*Institute of Organic Chemistry, Martin-Luther-University Halle, D-06120 Halle/Saale, Kurt-Mothes-Straße 2, Germany*
E-mail: coqfx@mlucom.urz.uni-halle.de

[b]*Institute of Physical Chemistry, Martin-Luther-University Halle, D-06099 Halle/Saale, Mühlpforte 1, Germany*

Novel liquid crystalline oligomesogens, which consist of five, six or eight calamitic 4-cyanobiphenyl, 2-alkyl-5-phenyl-1,3,4-thiadiazole or 5-octyl-2-phenylpyrimidine units covalently linked by spacers of different length with a cyclotribenzylene central core (CTV derivatives, 2,3,7,8,12,13-hexa-substituted 10,15-dihydro-5*H*-tribenzo[*a*,*d*,*g*]cyclononenes) or a cyclotetrabenzylene central core (CTTV derivatives, 2,3,6,7,10,11,14,15-octa-substituted 5,10,15,20-tetrahydrotetrabenzo[*a*,*d*,*g*,*j*]cyclododecenes) have been synthesized. These compounds were investigated by polarizing microscopy, differential scanning calorimetry and some of them were also studied by X-ray diffraction. Many of the CTV derivatives show liquid crystalline properties. The cyanobiphenyl derivatives incorporating long spacer units have enantiotropic S_A phases which can easily be supercooled. The thiadiazole derivatives and the pyrimidine derivatives have liquid crystalline phases only if the spacer units are rather short. Thiadiazole derivatives with an odd number of connecting atoms between the CTV core and the calamitic mesogens form S_A phases, whereas those with even-numbered spacers display columnar mesophases. We propose that the columnar mesophases observed for these oligomesogens do not result from their ability to adopt a nearly disc-like shape. Instead, they represent ribbon phases which result from a steric frustration caused by the different space filling of the central cone-like core and the rod-like mesogenic groups. A chevron-like (banana-like) average shape of the molecules with even-numbered spacers is assumed to be responsible for the formation of the ribbon phases.

Also a CTTV derivative with eight appended phenylthiadiazole mesogens displays a columnar mesophase. A nematic phase was found for the corresponding cyanobiphenyl derivative, whereas the pyrimidine derivative is not liquid crystalline.

Liquid crystalline materials have become increasingly important for many applications.[1] Besides their well-established application in electrooptical display devices, they are also interesting candidates for information storage, nonlinear optics[2] and photoconductivity.[3]

It is well known that thermotropic liquid crystalline phases may be formed by rod-like as well as by disc-shaped molecules. Thereby the molecular shape determines the kind of mesophase observed. Rod-like molecules give rise to nematic and/or lamellar liquid crystalline phases whereas flat discotic, on average disc-shaped and also cone-shaped molecules can self organize to give discotic nematic phases and/or columnar mesophases.[4]

The investigation of the transition between layered (smectic) and columnar liquid crystalline phases is a topic of current interest. New materials and novel mesophases with interesting properties (*e.g.* biaxial nematic[5] and cubic phases[6]) can be expected in this intermediate region. Initially, catenated molecules were designed to bridge the gap between these two different types of mesophases.[7] These molecules represent hybrid molecules with a long rod-like rigid core ending in two half-disc moieties and can exhibit nematic, lamellar and columnar phases. The covalent linkage of differently shaped molecules *via* spacer units is an alternative way to create new supramolecular structures.[8] This was first realized by Ringsdorf *et al.*, who connected two disc-like triphenylene units with a rigid core.[9]

We have recently reported the first cyclotriveratrylene (CTV) derivatives connected with five or six calamitic units.[10,11] We found that, depending on the length of the spacers connecting the central cone-shaped CTV-unit to the rod-like rigid cores, either columnar or smectic phases can be formed. If the calamitic unit was directly attached to the central unit *via* a carboxy group, then broad columnar mesophases were found (type **A**). Compounds in which the calamitic units are separated from the CTV-unit by spacers with a medium length (type **B**) form smectic A phases, whereas long spacers cause the loss of the mesogenic properties (type **C**). However, the materials reported so far have not only differed in spacer length, but also in the type of calamitic units incorporated and no systematic studies concerning the influence of the spacer length on the mesomorphic properties have been carried out.

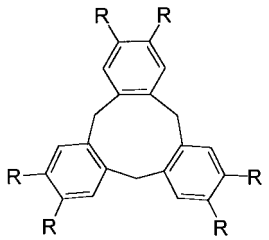

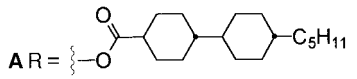

cr 118 °C Col 355 °C dec.

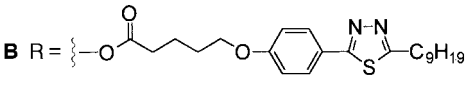

cr 152 °C S_A 160 °C is

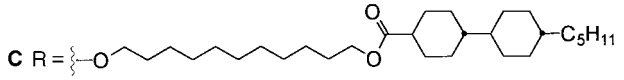

cr 115 °C is

Compounds with short spacers are of special interest because they represent borderline cases between materials forming lamellar and columnar phases.

Three types of rod-like rigid cores have been chosen for our investigations: 4-cyanobiphenyls, 2-phenylpyrimidines and 2-phenylthiadiazoles. These rigid cores differ in the direction of their dipole moments (along or perpendicular to the long molecular axis) and in the kind of mesophases formed by their simple alkyl derivatives (4-cyanobiphenyls: nematic, 2-phenylpyrimidines and 2-phenylthiadiazoles: smectic A and C).

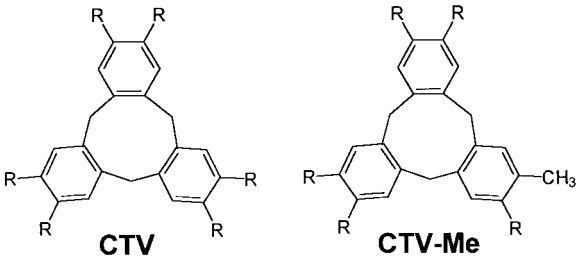

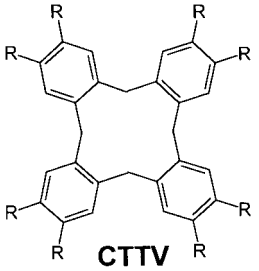

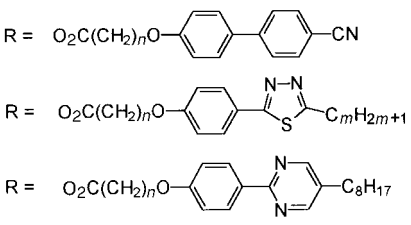

Also, two different types of disc-like central units have been used. The CTV unit is rigid but not strictly flat. Nevertheless, derivatives with a sufficiently large number of aliphatic chains connected to this cone-shaped central unit exhibit columnar mesophases (bowlic liquid crystals).[12,13] The possibility that these achiral compounds can form mesophases with ferroelectric properties is another interesting aspect which will not however be discussed here.[12,14] Cyclotetraveratrylene (CTTV) derivatives in contrast are much more flexible and can be regarded as being disc-shaped molecules on the average.[15] We hoped that the type of supermolecular arrangements could be influenced by combining these different calamitic and disc-like units. Here we report two homologous series of CTV derivatives in which six calamitic phenylthiadiazole or cyanobiphenyl rigid cores are fixed *via* flexible spacers of different length to the macrocyclic cyclotribenzylene unit. Additionally, two phenylpyrimidine derivatives have been prepared. Furthermore, we have synthesized selected asymmetric cyclotribenzylene derivatives carrying only five rigid cores and cyclotertrabenzylene derivatives (CTTV derivatives), even with eight appended rigid cores.

Synthesis

The synthesis of the symmetric CTV and CTTV derivatives was achieved by esterification[10,11,16] of cyclotricatechylene (2,3,7,8,12,13-hexahydroxy-10,15-dihydro-5*H*-tribenzo [*a*,*d*,*g*] cyclononene)[17] and cyclotetracatechylene (2,3,6,7,10,11,14,15-octahydroxy-5,10,15,20-tetrahydrotetrabenzo[*a*,*d*,*g*,*j*]cyclododecene)[13,18] respectively with appropriate carboxylic acids incorporating a 4′-cyanobiphenyl, a 5-phenylthiadiazole or a 5-phenylpyrimidine rigid core. As an example, the synthesis of the pyrimidine derivatives **5** and **9** is shown in Scheme 1.

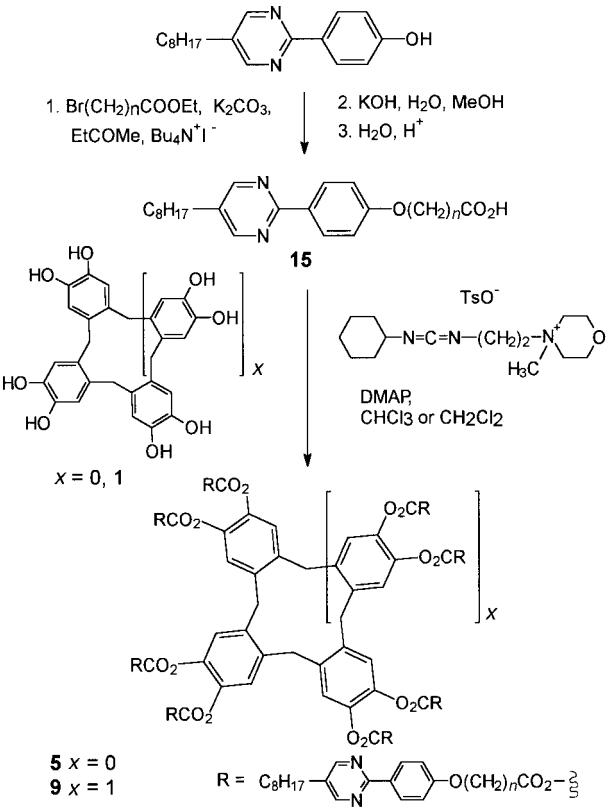

Scheme 1

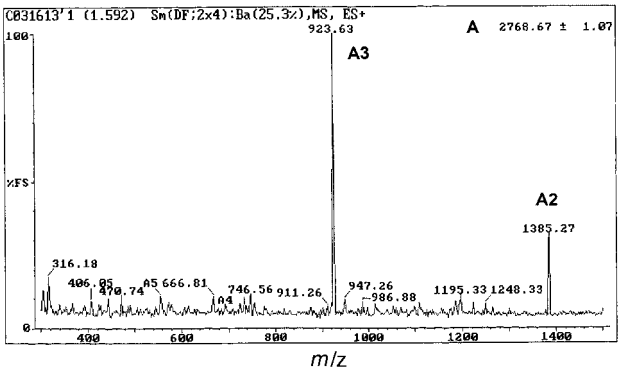

Fig. 1 Electrospray mass spectrum of compound **3e**

Cyclotricatechylene and cyclotetracatechylene were obtained according to standard procedures by cyclocondensation of veratrole with formaldehyde, followed by cleavage of the methyl ethers by means of boron tribromide.[13,17,18] For the synthesis of the asymmetric compounds a stepwise condensation procedure was used to prepare 2-methyl-3,7,8,12,13-pentahydroxy-10,15-dihydro-5*H*-tribenzo [*a*,*d*,*g*]cyclononene[17] which was esterified as described above. The structure of all final compounds was confirmed from their ^{1}H NMR spectra and combustion analysis. Furthermore electrospray–MS investigations indicate the correct molecular mass. Peaks for only partially acylated products were not detected (see for example Fig. 1).

Results and Discussion

We have studied systematically the dependence of the mesomorphic properties on spacer length. The transition temperatures and the corresponding enthalpy values of the cyclotribenzylene derivatives are summarized in Tables 1, 2 and 4.

4-Cyanobiphenyl derivatives

In the series of 4-cyanobiphenyl derivatives **1** the melting points and the clearing temperatures decrease with increasing chain length (Table 1). Thereby the decrease in the melting temperatures is more pronounced than the decrease in the clearing temperature. Owing to the high melting points of the compounds with short spacers no mesophases could be detected for compounds **1a** and **1c** and only monotropic phases were found for **1b** and **2a**. The other cyanobiphenyl derivatives with long chains (compounds **1d** and **1e**) display enantiotropic liquid crystalline properties.

All mesophases of the cyanobiphenyl derivatives show the same optical texture. On cooling, the appearance of a non-specific birefringent texture and homeotropically aligned regions were observed. On annealing these samples close to the clearing temperature, the formation of a focal conic fan texture could be observed.

The mesophase of compound **1b** was investigated using a Guinier goniometer. The typical diffraction pattern of a layered structure without order within the layers was observed. The layer thickness was calculated to be 3.03 nm. The length of the molecule is estimated (CPK models) to be about 4.5 nm. From this interdigitation of the cyanobiphenyl groups can be deduced. From the textural observations and from the X-ray pattern we conclude that a smectic A phase exists. Because the optical textures are identical for all investigated compounds **1**, it is reasonable to assume that all mesomorphic cyanobiphenyl derivatives **1** and **2** display S_A phases.

Comparison of these compounds with related monomeric 4-cyanobiphenyl liquid crystals (*e.g.* $C_6H_{13}O-C_6H_4-C_6H_4-CN$: Cr 57 °C N 75.5 °C I)[19] indicates that appending the cyanobiphenyl mesogens to the cyclotribenzylene unit gives rise to a significant mesophase stabilization and additionally the nematic phase of the monomeric 4-cyanobiphenyl derivatives is replaced by smectic A phases in the CTV derivatives **1**. This means that the cyclotribenzylene linking unit stabilizes a layered arrangement of the individual calamitic molecules. The clearing temperatures and also the melting points decrease by elongation of the spacers. Because the melting temperatures are more strongly influenced than the clearing temperatures, compounds with short spacers have monotropic mesophases and those with long spacers are enantiotropic liquid crystals. In the cases of compounds **1a** and **1c** it was not possible to supercool the samples to sufficiently low temperatures to allow the observation of liquid crystalline phases. However, compounds **1d** and **1e** with long spacer units form enantiotropic S_A phases which can easily be supercooled to −30 °C without crystallization. Crystallization occurs only after prolonged storage.† Sections of the DSC heating and cooling curves of compound **1d** are shown in Fig. 2.

Table 1 Phase transition temperatures[a] and transition enthalpies (lower lines) of the cyclotribenzylene derivatives **1** and **2**

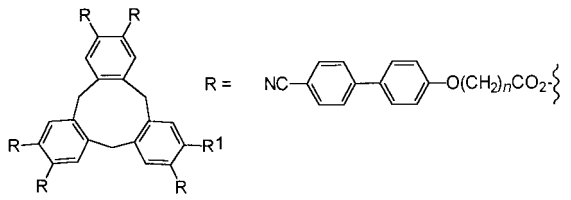

R^1	n	comp.	transition temperatures, T/°C *transition enthalpies,* ΔH/kJ mol^{-1}
R	3	**1a**	Cr 220 I *75.8*
R	4	**1b**[11]	Cr 165 (S_A 133) I *76.6* *6.6*
R	5	**1c**	Cr 159 I *83.9*
R	6	**1d**	Cr_1 65 Cr_2 112 S_A 123 I *18.8* *7.0* *8.2*
R	10	**1e**	Cr 95 S_A 116 I *58.3* *21.3*
CH_3	3	**2a**	Cr 163 (S_A 145) I *40.4*
CH_3	4	**2b**[11]	Cr 80 S_A 118 I
CH_3	10	**2c**	Cr 78 S_A 107 I *48.3* *18.1*

[a]Abbreviations: Cr = crystalline, S_A = smectic A-phase, I = isotropic phase.

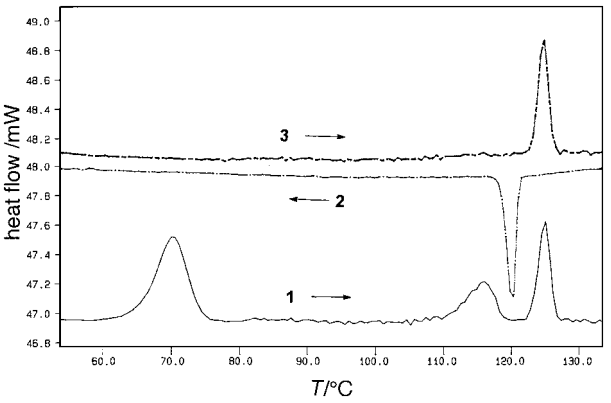

Fig. 2 DSC heating and cooling traces of compound **1d** (5 K min^{-1})

Replacing one of the rigid cores with a methyl group (compounds **2**) gives rise to a mesophase destabilization (*cf.* compound **1b** with six rigid cores and compound **2b** with only five rigid cores) and additionally, the melting points and the crystallization tendency are decreased by this desymmetrization of the molecules.[11] A monotropic S_A phase was observed by cooling the cyclotribenzylene derivative **2a** which is a desymmetrized analogue of the non-liquid crystalline compound **1a**. Compound **2a** with only five rigid cores, but with the shortest spacer length, has the most stable mesophase of all cyanobiphenyl derivatives investigated.

Thiadiazole derivatives

The phase behaviour of the thiadiazole derivatives **3** depends on the spacer length and differs significantly from that of the cyanobiphenyl compounds **1** (Table 2).

Again, the clearing temperatures decrease on elongation of the spacer units. However, the melting points of compounds **3** remain nearly constant. Therefore, in this series of compounds mesomorphic properties are only observed for the short chain derivatives and are lost on increasing the spacer length.

The optical textures of compounds **3a**, **3c**, **3i** and **4b** which have three or five methylene groups in the spacers differ from those of the compounds **3b**, **3g**, **3h** and **4a** with four methylene groups in the spacer units. The next homologue with six methylene units (compound **3d**) is only a crystalline solid. The liquid phase of **3d** can be supercooled to 145 °C and at this temperature no liquid crystalline phase is detected.

† Often, only part crystallization can be observed even after prolonged storage. This explains the low melting enthalpy values found for some compounds.

Table 2 Phase transition temperatures[a] and transition enthalpies (lower lines) of the cyclotribenzylene derivatives **3** and **4** incorporating a 2-phenylthiadiazole unit

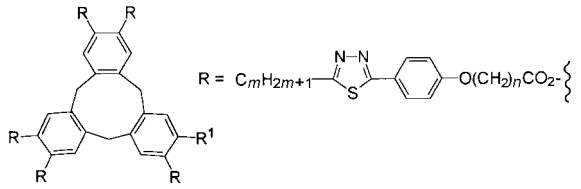

R[1]	*m*	*n*	comp.	transition temperatures, T/°C *transition enthalpies,* ΔH/kJ mol^{-1}					
R	7	3	**3a**	Cr	152	Col	182	I	
					10.7		*54.0*		
R	7	4	**3b**[11]	Cr	117	S_A	159	I	
R	7	5	**3c**	Cr	151	Col	155	I	
					30.6		*65.8*		
R	7	6	**3d**	Cr	156	I			
					144.9				
R	7	7	**3e**	Cr	158	I			
					135.6				
R	7	10	**3f**[11]	Cr	142	I			
R	9	4	**3g**[11]	Cr	152	S_A	160	I	
R	15	4	**3h**	Cr_1	102	Cr_2	143	S_A	155 I
					87.1		*0.9*		
R	9	5	**3i**	Cr	80	Col	162	I	
CH_3	9	4	**4a**[11]	Cr	<20	S_x	126	S_A	142 I
CH_3	9	5	**4b**	Cr	62	Col	148	I	

[a]Abbreviations: S_x = unknown smectic phase, Col = columnar mesophase.

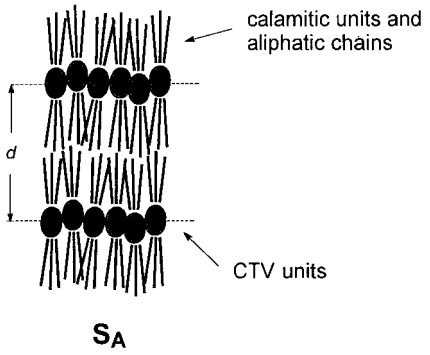

Fig. 3 Model of the S_A phase of compound **3b**, **3g** and **3h**

Smectic phases of thiadiazole derivatives. The above mentioned compounds with an even number of methylene groups (*i.e.* with an odd total number of connecting atoms in each spacer, because of the ether oxygen and the carboxy group) show small focal conic fan-textures, which can be homeotropically aligned on shearing the samples to give optically isotropic regions. These textural features are typical for S_A phases. The X-ray patterns of compounds **3b** and **4a** have been discussed in a recent paper[11] and confirm a smectic layer structure without order in the layers. The layer period in the S_A phase of compound **3g** is 5.3 nm. The molecules can be considered as oligomesogens consisting of rod-like rigid cores appended to the CTV central unit with an average double forked conformation. Assuming this conformation, the molecular length in the most extended form (CPK models) is 6.3 nm. With respect to the calamitic phenylthiadiazole mesogens, these smectic phases can be regarded as bilayer structures which are formed by the segregation of the central CTV units from the terminal aliphatic chains (Fig. 3).

Columnar mesophases of thiadiazole derivatives. The thiadiazole derivatives **3a**, **3c**, **3i** and **4b** which have an odd number of methylene groups (*i.e.* with an even total number of connecting atoms in each spacer) differ significantly from the compounds discussed above. They form highly viscous mesophases and display spherulitic flower textures which are typical of columnar mesophases (see Fig. 4).

The mesophases of compounds **3a** and **3c** were investigated by X-ray diffraction using a Guinier film camera. Both compounds have a diffuse scattering in the wide angle region. Therefore a higher ordered smectic mesophase can be excluded. Additionally, besides a strong scattering there are several scatterings of low intensity in the small angle region. Table 3 displays the observed reflections of compound **3a**, which have been evaluated on the basis of an oblique cell. The resulting lattice parameters are $a = 5.6$, $b = 2.26$ nm and $\beta = 48°$.

To propose a model for the arrangement of the molecules in this columnar phase, different molecular conformations have to be considered. The CPK models of three possible conformations of compound **3a** are shown in Fig. 5. The star-shaped conformation [Fig. 5(*a*)] cannot explain the observed lattice parameters. If the averaged molecules exist in a stretched double forked conformation with three calamitic units placed side by side [Fig. 5(*b*)], then their total length in the most

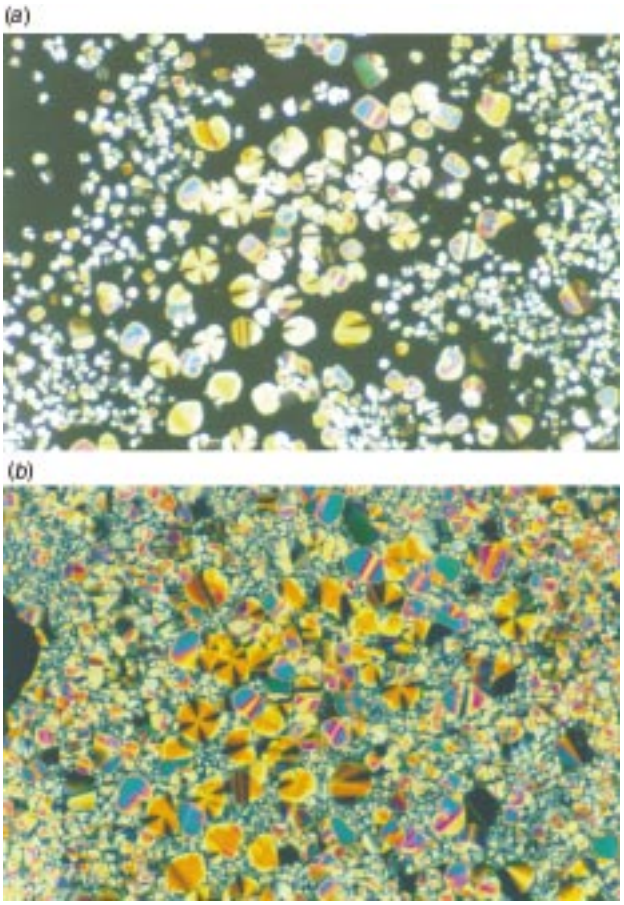

Fig. 4 Optical textures of the thiadiazole derivative **3a** as obtained by cooling from the isotropic melt (crossed polarizers): (*a*) transition I–Col at 182 °C; (*b*) Col phase at 170 °C

Table 3 Lattice parameter of the mesophase of compound **3a** at $T = 170$ °C

no.	Θ_{exp}	*hk*
1	1.05	10
2	2.07	11
3	2.61	01
4	3.11	30
5	3.69	32

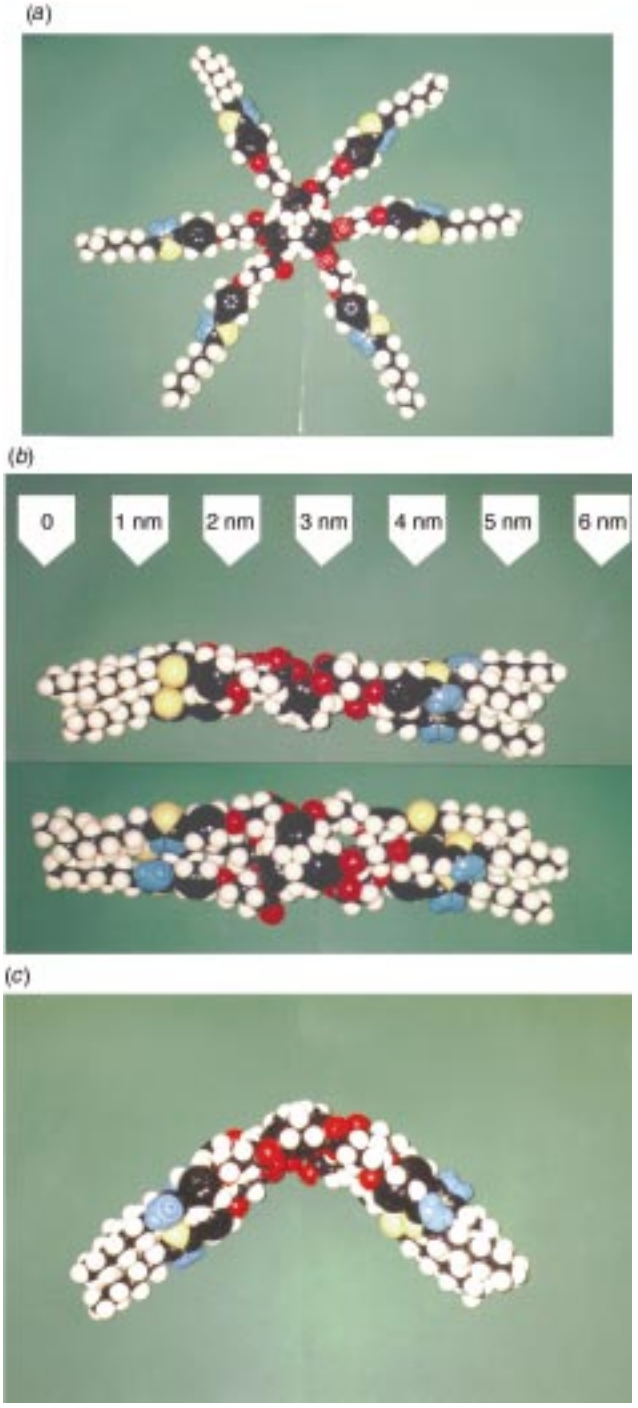

Fig. 5 Structure of compound **3a**: (*a*) fully stretched (star-shaped) conformation; (*b*) double-forked structure showing aligned rigid cores (side view and top view); (*c*) chevron-shaped conformation (side view)

extended conformation is *ca.* 5.7 nm, which agrees well with the lattice parameter $a = 5.6$ nm. However, in order to realize this conformation the cone-like shape of the CTV unit must be compensated for by a bend in the spacer units. In the third conformation [Fig. 5(*c*)] a chevron-like molecular shape is proposed. It should be provided by the cone-like shape of the CTV unit and is transferred to the total shape of the molecules by the even-numbered spacers. Interestingly, the angle $\beta = 48^\circ$ of the oblique lattice of the columnar phase of **3a** corresponds exactly to the angle $\phi = 47 \pm 2^\circ$ between the C_3-axis and the planes of the benzene rings of the CTV unit (see Fig. 6).[20]

A possible model of the columnar phase based on a chevron-like average conformation of compound **3a** is sketched in Fig. 6. This columnar phase can be regarded as a two-dimensional arrangement of ribbons which are extended in the third dimension (ribbon-phase).

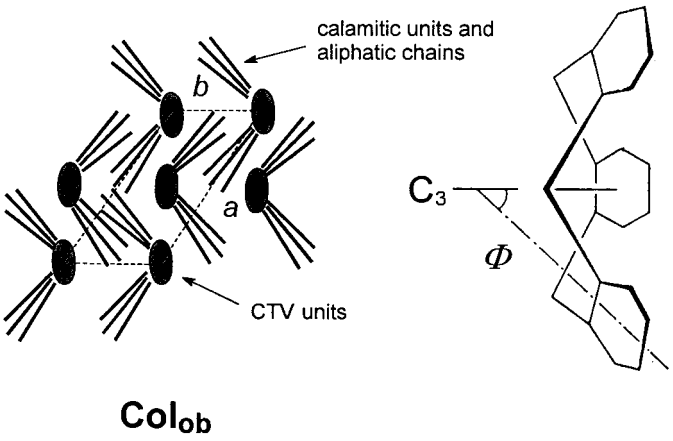

Fig. 6 Structure of the CTV central unit (right-hand side) and possible packing model of the molecules of compound **3a** in the ribbon phase (left-hand side)

According to this structure, the lattice parameter *a* should be equal to twice the length of the mesogenic units (2.4 nm) plus the diameter of the CTV unit (1.0 nm).‡ The observed lattice parameter $a = 5.6$ nm is in excellent agreement with this molecular parameter. The angle $\beta = 48^\circ$ of the oblique lattice is provided by the angle $\phi = 47 \pm 2^\circ$ between the planes of the benzene rings of the CTV unit and the C_3-axis of the CTV unit,[20] which is orientated parallel to *b*. Assuming two molecules per unit cell and considering the tilt of the molecular moieties, then the value of the parameter *b* can also be well understood. Considering the mesogenic groups as structural units, which are linked *via* the CTV moieties, then the ribbons can be regarded as one-dimensionally extended fragments of a smectic bilayer.

Such a ribbon arrangement, which partly destroys the natural segregation between the aromatic CTV units and the alkane chains must be favoured for geometric reasons. The different space filling of the CTV unit and the spacers on the one hand and the calamitic mesogens with their appended alkyl chains on the other are likely responsible for the destabilization of the layer-like organization of the molecules and give rise to the formation of ribbons. This model of the columnar mesophase is related to other two-dimensional modulated phases.[21–30] Modulated phases were also detected for terminally connected dimesogens.[31–33]§ In this case an alternation of the mesomorphic behaviour with the parity of the spacer length was found. When the total number of atoms in the spacer is even, the molecules adopt a rod-like shape and form smectic phases. When this number is odd, the dimesogens have a bent average conformation. The formation of antiferroelectrically ordered and modulated phases is then favoured.

An alternation of the mesomorphic properties with the parity of the spacer length is also found for the CTV derivatives synthesized by us (see above).¶ In our case however, spacers with an odd total number of connecting atoms can partly compensate for the bent structure of the CTV unit and give rise to a more rod-like total shape [see Fig. 5(*b*)] which favours smectic phases. The chevron-like molecular shape provided by

‡ This roughly corresponds to the molecular length in the biforked conformation [Fig. 5(*b*)].

§ In this respect some unusual features of nematic and smectic phases of terminally connected oligomesogens, such as cyclotriphosphazenes,[38] oligosiloxanes[39] and cyclohexane 1,3,5-tricarboxylates[40] are under discussion.

¶ Because only three homologues are liquid crystalline, the question remains open as to whether this odd–even parity is also valid for the higher homologues.

the even-numbered spacers favours the formation of ribbon phases. Thus the cone-like shape of the CTV linking unit provides an inverted odd–even parity in comparison to dimesogens.

Pyrimidine derivatives

Three 2-phenylpyrimidine derivatives have been synthesized. Compound **5a** exhibits liquid crystalline properties in the temperature range between 143 and 177 °C, whereas the next homologue **5b** is only a crystalline solid (Table 4).

It seems that the dependence of the mesophase stability on the spacer length is analogous to that of the thiadiazole derivatives, *i.e.* decreasing mesophase stability is observed on elongation of the spacers. However, in the case of the pyrimidine derivatives the melting temperatures are significantly higher and therefore the mesogenic properties are lost in the tetramethylene derivative **5b**. Even desymmetrization of the molecule by replacing one mesogenic unit by a methyl group (compound **6**) cannot give rise to liquid crystalline properties.

The mesophase behaviour of compound **5a** is rather interesting because a phase transition occurs within the mesomorphic range at a temperature of 170 °C. The high temperature mesophase shows a spherulitic flower texture [Fig. 7(*a*)], which is similar to the texture observed for the columnar mesophases of the thiadiazole derivatives (see Fig. 4). However the X-ray pattern displays only a layer reflection with a periodicity of 2.9 nm and a diffuse halo in the wide angle region. It is remarkable that the observed periodicity corresponds only to half the total molecular length [$L = 5.9$ nm, CPK model in the most extended conformation similar to Fig. 5(*b*)], which supports a smectic 'monolayer' structure.

At the transition to the low temperature mesophase the texture becomes broken and nonspecific as shown in Fig. 7(*b*). Here the X-ray studies suggest an oblique cell with $a = 5.82$, $b = 2.27$ nm, $\beta = 47.4°$. The diffuse halo in the wide angle region is maintained. The parameter a corresponds to the molecular length, whereas the parameters b and β are nearly identical to the corresponding parameters of the thiadiazole derivative **3a**. Therefore, the same ribbon model as for compound **3a** can be discussed for the low temperature mesophase of the pyrimidine derivative **5a**.

A possible model for the high temperature phase is based on the assumption that increasing the temperature can lower the steric frustration between terminal chains and CTV units and therefore give rise to a partial segregation of the CTV units from the alkyl chains. The aggregation of the CTV units

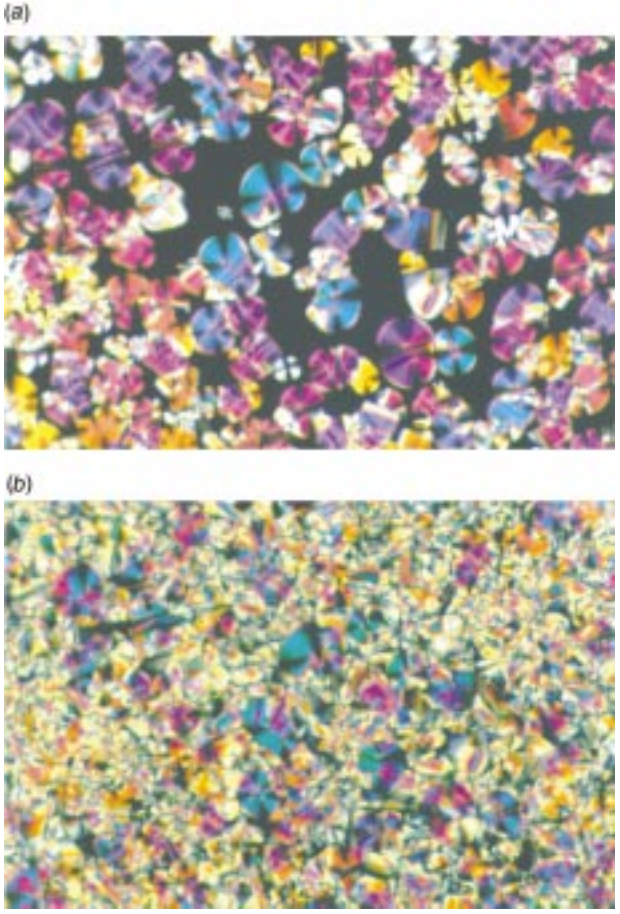

Fig. 7 Optical textures (crossed polarizers) of the 2-phenylpyrimidine derivative **5a** as obtained by cooling from the isotropic melt: (*a*) transition I–M at 177 °C; (*b*) transition M–Col at 170 °C

can lead to an enlarged and non-uniform diameter of the ribbons (more than one molecule is found in the diameter of the ribbons). The well-defined oblique lattice is lost and only a layer-like scattering corresponding to approximately half the molecular length remains. If this is valid, the M phase should also be a ribbon phase; only a layer reflection can be seen in the X-ray diffraction pattern, however, suggesting a smectic layer structure.

Table 4 Phase transition temperatures[a] and transition enthalpies (lower lines) of the pyrimidine derivatives **5** and **6**

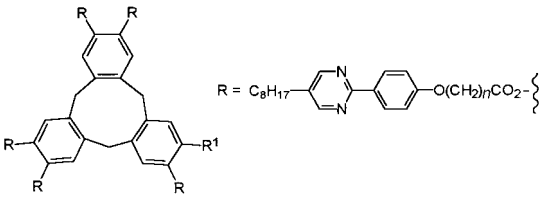

R^1	n	comp.	transition temperatures, T/°C *transition enthalpies,* ΔH/kJ mol^{-1}
R	3	**5a**	Cr 143 Col 170 M 177 I *7.4* *32.4* *22.2*
R	4	**5b**	Cr 168 I *84.6*
CH_3	4	**6**	Cr_1 126 Cr_2 138 I *20.6* *70.3*

[a]Abbreviations: M = unknown liquid crystalline phase.

CTTV derivatives

The mesomorphic properties of the synthesized CTTV derivatives **7**–**9** are summarized in Table 5. In contrast to the CTV derivatives **1**, which have S_A phases, the cyanobiphenyl derivative **7** is a nematic liquid crystal as is obvious from the typical nematic schlieren texture.

A spherulitic texture was observed for the thiadiazole derivative **8** on cooling from the isotropic melt (Fig. 8). From this texture we can conclude that an S_A phase is absent. This mesophase could possibly be a columnar phase (ribbon phase). However, the high melting temperature and the onset of decomposition at temperatures above 200 °C does not allow the X-ray investigations of this mesophase and therefore no confirmation of the phase structure was possible.

The pyrimidine derivative **9** is a crystalline solid with no mesophase.

Interestingly, in the case of the CTTV derivatives, columnar mesophases can be observed for compounds with an odd number of connecting atoms in the spacers. Because the CTTV unit adopts an averaged disc-like shape rather than a bowl-like shape, this observation is in accordance with the proposed model. The odd–even parity is possibly inverted for the CTTV

Table 5 Phase transition temperatures[a] and transition enthalpies (lower lines) of the CTTV derivatives **7–9**

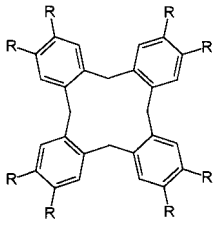

R	comp.	transition temperatures, T/°C *transition enthalpies,* ΔH/kJ mol^{-1}
$O_2C(CH_2)_3O$–⟨⟩–⟨⟩–CN	**7**	Cr_1 174 Cr_2 222 (N 220) I *53.8* *63.6*
$O_2C(CH_2)_4O$–⟨⟩–⟨N–N, S⟩–C_9H_{19}	**8**	Cr_1 142 Cr_2 204 M 222 I *70.3* *10.6* *44.5*
$O_2C(CH_2)_4O$–⟨⟩–⟨N, N⟩–C_8H_{17}	**9**	Cr 241 I

[a]Abbreviations: N = nematic phase.

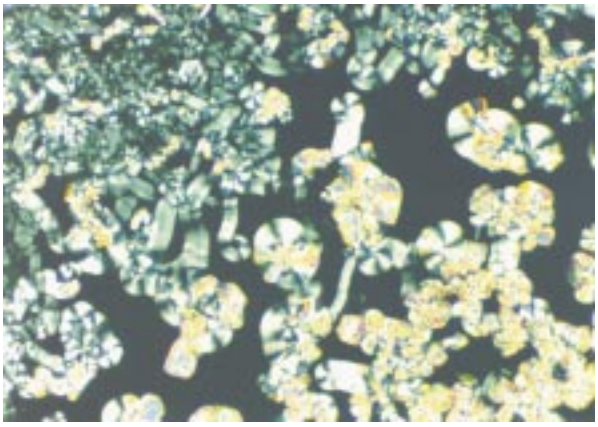

Fig. 8 Optical photomicrograph of the mesophases of the CTTV derivative **8** (crossed polarizers) as obtained by cooling from the isotropic melt at 222 °C

derivatives. Unfortunately no liquid crystalline CTTV derivatives with even numbered spacer units have been obtained.

Summary

In conclusion, we have prepared liquid crystalline oligomesogens which consists of five, six and even eight calamitic 4-cyanobiphenyl, 2-alkyl-5-phenyl-1,3,4-thiadiazole or 5-octyl-2-phenylpyrimidine units covalently linked by spacers of different lengths with cyclotribenzylene or cyclotetrabenzylene central cores. The cyanobiphenyl derivatives incorporating the CTV unit have broad S_A phases which can easily be supercooled if the spacer units are long. The thiadiazole derivatives and the pyrimidine derivatives have liquid crystalline phases only if the spacer units are rather short. Phenylthiadiazole substituted CTV derivatives with an odd number of connecting atoms form S_A phases. With respect to the calamitic phenylthiadiazole mesogens, these smectic phases can be regarded as bilayer structures which are formed by the segregation of the central CTV units from the terminal aliphatic chains.

Columnar mesophases were found for those compounds in which phenylthiadiazoles and phenylpyrimidines were appended *via* even numbered spacers to a CTV unit and for phenylthiadiazole derivatives grafted to CTTV units. We propose that the columnar mesophases observed for these oligomesogens are not the result of the ability to adopt a disc-like shape. Rather, they represent ribbon phases which arise from the steric frustration caused by the different space filling of the central cone-like core and the attached rod-like mesogens. A chevron-like average shape of the molecules with even-numbered spacers is assumed to facilitate this steric frustration and be responsible for the formation of the ribbon phases. Odd-numbered spacers can partly compensate for the bent structure of the CTV unit and give rise to S_A phases.

A nematic phase was only found in the case of a CTTV derivative with appended cyanobiphenyl mesogens. Thus, the covalent fixation of calamitic mesogens to central connecting units can not only stabilize smectic mesophases but also provide the possibility to change the phase structure of calamitic mesogens from smectic to columnar with only minor adjustments of the chemical structure. The ability of these molecules to adopt a chevron-shaped (banana-shaped) geometry is of special interest with respect to potential ferroelectric properties.[34] Furthermore, the special kind of mesophases found in the so-called banana-shaped molecules[34] could be related to the ribbon-phases described here.

Experimental

Methods

Confirmation of the structures of intermediates and products was obtained by ^{1}H and ^{13}C NMR spectroscopy (Bruker WP 200 spectrometer and a Varian Unity 500; coupling constants J are given in Hz), infrared spectroscopy (Specord 71 IR) and mass spectrometry (Intectra GmbH, AMD 402, electron impact, 70 eV; electrospray–MS, VG Bio-Q Fisons Instruments). Microanalyses were performed using an Carlo-Erba 1102 or a Leco CHNS-932 elemental analyser. Transition temperatures were measured using a Mettler FP 82 HT hot stage and control unit in conjunction with a Nikon Optiphot 2 polarizing microscope and these were confirmed using differential scanning calorimetry (Perkin-Elmer DSC-7). X-Ray studies were performed using a Guinier goniometer (Fa. Huber).

Materials

4-(5-Alkyl-1,3,4-thiadiazol-2-yl)phenols[35] and 4-(5-octylpyrimidin-2-yl)phenol,[36] 3,7,8,12,13-hexahydroxy-10,15-dihydro-5*H*-tribenzo[*a*,*d*,*g*]cyclononene,[17] 3,7,8,12,13-pentahydroxy-2-methyl-10,15-dihydro-5*H*-tribenzo[*a*,*d*,*g*]cyclononene[11] and 2,3,6,7,10,11,14,15-octahydroxy-5,10,15,20-tetrahydrotetrabenzo-[*a*,*d*,*g*,*j*]cyclododecene[18] were synthesized according to literature procedures. 4-(4-Cyanophenyl)phenol and 11-bromoundecanoic acid were obtained from Merck. The methyl and ethyl ω-bromoalkanoates (Aldrich) were used as obtained. Methyl 7-bromoheptanoate was synthesized from 6-bromohexanoic acid *via* chain elongation with diazomethane.[37]

Alkyl ω-[4-(4-cyanophenyl)phenoxy]alkanoates 10, alkyl ω-[4-(5-alkyl-1,3,4-thiadiazol-2-yl)phenoxy]alkanoates 12 and ethyl ω-[4-(5-octylpyrimidin-2-yl)-phenoxy]alkanoates 14. 4-(4-Cyanophenyl)phenol, 4-(5-alkyl-1,3,4-thiadiazol-2-yl)phenol or 4-(5-octylpyrimidin-2-yl)phenol (20 mmol) was dissolved in dry butan-2-one (200 ml), the appropriate alkyl ω-bromoalkanoate (40 mmol), K_2CO_3 (8.3 g, 60 mmol) and tetrabutylammonium iodide (50 mg) were added and the resulting mixture was stirred at reflux temperature until the phenol could not be detected by TLC (1–10 h). After cooling, the solvent was evaporated and the residue was dissolved in water (50 ml) and dichloromethane (100 ml). The organic phase was washed with sodium hydrogen carbonate (50 ml), hydrochloric acid (10%, 50 ml) and water (50 ml) successively. Afterwards the solution was dried with Na_2SO_4 and the solvent was removed *in vacuo*. The 4-cyanobiphenyl derivatives **10** and the

thiadiazole derivatives **12** were crystallized twice from light petroleum (bp 60–85 °C)–ethyl acetate. The pyrimidine derivatives **14** were crystallized from ethanol. The transition temperatures of the compounds **10**, **12** and **14** are summarized in Tables 6–8. Analytical data of the compounds **10a**, **12a** and **14a** are given as representative examples.

Ethyl 4-[4-(4-*cyanophenyl*) *phenoxy*]*butanoate* **10a**. Elemental analysis (%): found (calc. for $C_{19}H_{19}NO_3$): C, 73.46 (73.77); H, 5.96 (6.19); N, 4.52 (4.53). δ_H ($CDCl_3$) 1.26 (m, 6H, CH_3), 2.15 (m, 2H, CH_2), 2.54 (t, 2H, *J* 7.2, CH_2COO), 4.05 (t, 2H, *J* 6.1, OCH_2CH_2), 4.15 (q, 2H, OCH_2CH_3), 6.99 (d, 2H, *J* 8.8, Ar-H), 7.52 (d, 2H, *J* 8.8, Ar-H), 7.62–7.75 (m, 4H, Ar-H).

Ethyl 4-[4-(5-*heptyl*-1,3,4-*thiadiazol*-2-*yl*)*phenoxy*]*butanoate* **12a**. Elemental analysis (%): found (calc. for $C_{21}H_{30}N_2O_3S$): C, 64.79 (64.59); H, 7.75 (7.74); N, 7.25 (7.17); S, 8.27 (8.21). δ_H ($CDCl_3$) 0.86 (m, 6H, CH_3), 1.23–1.8 (m, 10H, CH_2), 2.12 (m, 2H, CH_2), 2.5 (t, 2H, *J* 7.3, CH_2COO), 3.08 (t, 2H, *J* 7.7, $ArCH_2$), 4.05 (t, 2H, *J* 6.1, OCH_2CH_2), 4.13 (q, 2H *J* 7.1, OCH_2CH_3), 6.93 (d, 2H, *J* 8.85, Ar-H), 7.83 (d, 2H, *J* 8.85, Ar-H).

Ethyl 4-[4-(5-*octylpyrimidin*-2-*yl*)*phenoxy*]*butanoate* **14a**. δ_H ($CDCl_3$) 0.86 (m, 6H, CH_3), 1.15–2.11 (m, 14H, CH_2), 2.52 (t, 2H, *J* 7.2, CH_2COO), 2.58 (t, 2H, $ArCH_2$, *J* 7.7), 4.07 (t, 2H, *J* 6.1, OCH_2CH_2), 4.14 (q, 2H, *J* 7.2, CH_2CH_3), 6.95 (d, 2H, *J* 8.9, Ar-H), 8.32 (d, 2H, *J* 8.9, Ar-H), 8.55 (s, 2H, Ar-H).

ω-[4-(4-Cyanophenyl)phenoxy]alkanoic acids 11, ω-[4-(5-alkyl-1,3,4-thiadiazol-2-yl)phenoxy]alkanoic acids 13, and ω-[4-(5-octylpyrimidin-2-yl)phenoxy]alkanoic acids 15. The compounds **10**, **12** or **14** (10 mmol) were dissolved in methanol (150 ml) and heated to reflux. A solution of potassium hydroxide (1.7 g, 30 mmol) in water (20 ml) was added under stirring and the solution was refluxed for 2 h in the cases of **12** and **14** and only for 5 min in the case of compound **10**. After cooling, the mixture was poured on crushed ice. The precipitate which formed on acidification with dilute hydrochloric acid was filtered off, washed with water and crystallized twice from light petroleum (bp 60–85 °C)–ethyl acetate. The transition temperatures of the compounds **11**, **13** and **15** are summarized in the Tables 6–8. Analytical data of the compounds **11a**, **13a** and **15a** are given as representative examples.

Table 6 Phase transition temperatures of the ω-[4-(4-cyanophenyl)-phenoxy]alkanoic acids **11** and their alkyl esters **10**

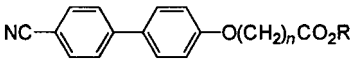

n	R	comp.	mp *T*/°C	R	comp.	phase transition temperatures *T*/°C
3	C_2H_5	**10a**	76	H	**11a**	Cr 200 (N 192) I
5	C_2H_5	**10b**	89–90	H	**11b**	Cr 173 (N 170) I
6	CH_3	**10c**	103	H	**11c**	Cr 123 (N 118) I
10	CH_3	**10d**	104	H	**11d**	Cr 129 (N 122) I

Table 8 Phase transition temperatures of the ω-[-4-(5-octylpyrimidin-2-yl)phenoxy]alkanoic acids **15** and their ethyl esters **14**

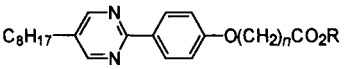

n	R	comp.	phase transition temperatures *T*/°C	R	comp.	mp *T*/°C
3	C_2H_5	**14a**	Cr 51 (S_A 44) I	H	**15a**	137
4	C_2H_5	**14b**	Cr 41 N 43 I	H	**15b**	117

4-[4-(4-*Cyanophenyl*)*phenoxy*]*butanoic acid* **11a**. Elemental analysis (%): found (calc. for $C_{17}H_{15}NO_3$): C, 72.30 (72.58); H, 5.61 (5.37); N, 4.74 (4.98). δ_H ($CDCl_3$) 2.15 (m, 2H, CH_2), 2.60 (t, 2H, *J* 7.2, CH_2COO), 4.07 (t, 2H, *J* 5.9, OCH_2CH_2), 6.97 (d, 2H, *J* 8.8, Ar-H), 7.50 (d, 2H, *J* 8.8, Ar-H), 7.61 (d, 2H, *J* 8.55, Ar-H), 7.67 (d, 2H, *J* 8.55, Ar-H). MS *m*/*z* (relative intensity, %): 281 (26, M^+), 228 (15), 195 (100), 166 (18), 151 (5), 140 (12), 101 (11), 87 (8).

4-[4-(5-*Heptyl*-1,3,4-*thiadiazol*-2-*yl*)*phenoxy*]*butanoic acid* **13a**. Elemental analysis (%): found (calc. for $C_{19}H_{26}N_2O_3S$): C, 63.01 (62.96) H, 7.27 (7.23); N, 7.72 (7.73); S, 8.91 (8.84). δ_H ($CDCl_3$): 0.86 (t, 3H, *J* 7, CH_3), 1.23–1.8 (m, 10H, CH_2), 2.12 (m, 2H, CH_2), 2.59 (t, 2H, *J* 7.2, CH_2COO), 3.09 (t, 2H, *J* 7.6, $ArCH_2$), 4.07 (t, 2H, *J* 6.1, OCH_2CH_2), 6.94 (d, 2H, *J* 8.7, Ar-H), 7.84 (d, 2H, *J* 8.7, Ar-H). δ_C ($CDCl_3$) 178, 169.8, 168.2, 161, 129.4, 123.2, 115, 66.8, 31.6, 30.3, 30.2, 30.1, 28.9, 28.8, 24.3, 22.6, 14. MS *m*/*z* (relative intensity, %): 362 (84, M^+), 347 (8, $M^+ - CH_3$), 333 (34), 319 (32), 305 (12), 291 (92), 278 (100), 247 (8), 233 (6), 219 (4), 205 (18), 192 (55), 137 (8).

4-[4-(5-*Octylpyrimidin*-2-*yl*)*phenoxy*]*butanoic acid* **15a**. δ_H ($CDCl_3$) 0.85 (t, 3H, *J* 6.4, CH_3), 1.2–1.7 (m, 14H, CH_2), 2.52–2.67 (m, 4H, CH_2), 4.08 (t, 2H, *J* 6.05, OCH_2CH_2), 6.95 (d, 2H, *J* 8.3, Ar-H), 8.31 (d, 2H, *J* 8.8, Ar-H), 8.56 (s, 2H, Ar-H). δ_C ($CDCl_3$): 177.8, 162.4, 160.7, 156.9, 132.2, 130.4, 129.5, 114.5, 66.7, 31.8, 30.8, 30.4, 30.2, 29.3, 29.2, 29.1, 24.5, 22.6, 14.1. MS *m*/*z* (relative intensity, %): 370 (38, M^+), 284 (100), 241 (5), 227 (10), 213 (6), 199 (31), 185 (74), 158 (11), 119 (4).

Esterification of the polyphenols. 2,3,7,8,12,13-Hexahydroxy-10,15-dihydro-5*H*-tribenzo[*a*,*d*,*g*]cyclononene, 3,7,8,12,13-pentahydroxy-2-methyl-10,15-dihydro 5*H*-tribenzo[*a*,*d*,*g*]-

Table 7 Phase transition temperatures of the ω–4-(5-alkyl-1,3,4-thiadiazol-2-yl)phenoxy]alkanoic acids **13** and their alkyl esters **12**

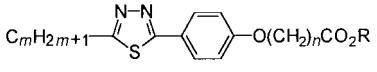

m	*n*	R	comp.	phase transition temperatures *T*/°C	R	comp.	mp *T*/°C
7	3	C_2H_5	**12a**	Cr 67 (S_A 63) I	H	**13a**	123
7	5	C_2H_5	**12b**	Cr 64 I	H	**13b**	113
7	6	CH_3	**12c**	Cr 58 I	H	**13c**	99
7	7	CH_3	**12d**	Cr 59 I	H	**13d**	107
15	4	C_2H_5	**12e**	Cr 78 I	H	**13e**	116

cyclononene or 2,3,6,7,10,11,14,15-octahydroxy-5,10,15,20-octahydrotetrabenzo[*a*,*d*,*g*,*j*]cyclododecene (0.2 mmol) and *N*-cyclohexyl-*N'*-[2-(*N*-methylmorpholinio)ethyl]carbodiimide toluene-*p*-sulfonate (1.5 equiv. per OH group) were dissolved in 50 ml of dry chloroform. After 5 min the appropriate substituted alkanoic acids **11**, **13** or **15** (1.3 equiv. per OH group) was added followed by addition of 4-(dimethylamino)pyridine (40 mg). The resulting mixture was stirred at room temp. for 20 h. After the reaction was complete, water (50 ml) was added to the mixture, and the phases were separated. The aqueous phase was extracted with $CHCl_3$ (30 ml). The combined organic phase was washed successively with saturated aqueous sodium hydrogen carbonate (30 ml), brine (30 ml), and water (30 ml). Afterwards, the solution was dried (Na_2SO_4) and the solvent was removed *in vacuo*. The products were purified by column chromatography using chloroform–methanol (25 : 1) followed by crystallization from nitromethane.

2, 3, 7, 8, 12, 13-*Hexakis*{4-[4-(4-*cyanophenyl*)*phenoxy*]*butanoyloxy*}-10,15-*dihydro*-5H-*tribenzo*[a,d,g]*cyclononene* **1a**. Yield: 73%, mp 220 °C. Elemental analysis (%): found (calc. for $C_{123}H_{96}N_6O_{18}$): C, 75.56 (75.91); H, 5.05 (4.97); N, 3.94 (4.32). δ_H ($CDCl_3$) 1.32–2.12 (m, 12H, CH_2), 2.66 (t, 12H, *J* 6.95, CH_2COO), 3.69 (d, 3H, *J* 14.2, $ArCH_2Ar$, H_e), 4.0 (t, 12H, *J* 5.9, OCH_2CH_2), 4.76 (d, 3H, *J* 13.55, $ArCH_2Ar$, H_a), 6.91 (d, 12H, *J* 8.8, Ar-H), 7.14 (s, 6H, Ar-H), 7.45 (d, 12H, *J* 8.75, Ar-H), 7.56 (d, 12H, *J* 8.4, Ar-H), 7.64 (d, 12H, *J* 8.4, Ar-H).

2, 3, 7, 8, 12, 13-*Hexakis*{6-[4-(4-*cyanophenyl*)*phenoxy*]*hexanoyloxy*}-10,15-*dihydro*-5H-*tribenzo*[a,d,g]*cyclononene* **1c**. Yield: 85%, mp 159 °C. Elemental analysis (%): found (calc. for $C_{135}H_{120}N_6O_{18}$): C, 76.43 (76.69); H, 5.64 (5.72); N, 4.21 (3.97). δ_H ($CDCl_3$) 1.53–1.86 (m, 36H, CH_2), 2.57 (t, 12H, *J* 6.6, CH_2COO), 3.74 (d, 3H, *J* 13.4, $ArCH_2Ar$, H_e), 4.01 (t, 12H, *J* 5.9, OCH_2CH_2), 4.81 (d, 3H, *J* 13.45, $ArCH_2Ar$, H_a), 6.99 (d, 12H, *J* 8.6, Ar-H), 7.19 (s, 6H, Ar-H), 7.53 (d, 12H, *J* 8.55, Ar-H), 7.64 (d, 12H, *J* 8.35, Ar-H), 7.69 (d, 12H, *J* 8.2, Ar-H).

2, 3, 7, 8, 12, 13-*Hexakis*{7-[4-(4-*cyanophenyl*)*phenoxy*]*heptanoyloxy*}-10,15-*dihydro*-5H-*tribenzo*[a,d,g]*cyclononene* **1d**. Yield: 40%, phase transitions (°C): Cr_1 65 Cr_2 112 S_A 123 I. Elemental analysis (%): found (calc. for $C_{141}H_{132}N_6O_{18}$): C, 76.93 (77.03); H, 6.14 (6.05); N, 3.73 (3.82). δ_H ($CDCl_3$) 1.3–1.84 (m, 48H, CH_2), 2.49 (t, 12H, *J* 7.35, CH_2COO), 3.67 (d, 3H, *J* 14.1, $ArCH_2Ar$, H_e), 3.95 (t, 12H, *J* 6.35, OCH_2CH_2), 4.73 (d, 3H, *J* 13.3, $ArCH_2Ar$, H_a), 6.92 (d, 12H, *J* 8.9, Ar-H), 7.12 (s, 6H, Ar-H), 7.47 (d, 12H, *J* 8.8, Ar-H), 7.6–7.7 (m, 24H, Ar-H).

2, 3, 7, 8, 12, 13-*Hexakis*{11-[4-(4-*cyanophenyl*)*phenoxy*]*undecanoyloxy*}-10,15-*dihydro*-5H-*tribenzo*[a,d,g]*cyclononene* **1e**. Yield: 45%, phase transitions (°C): Cr 95 S_A 116 I. Elemental analysis (%): found (calc. for $C_{165}H_{180}N_6O_{18}$): C, 78.50 (78.17); H, 7.23 (7.16); N, 3.21 (3.31). δ_H ($CDCl_3$) 1.2–1.84 (m, 96H, CH_2), 2.45 (t, 12H, *J* 7.4, CH_2COO), 3.65 (d, 3H, *J* 14.1, $ArCH_2Ar$, H_e), 3.96 (t, 12H, *J* 6.51, OCH_2CH_2), 4.72 (d, 3H, *J* 14.3, $ArCH_2Ar$, H_a), 6.94 (d, 12H, *J* 8.8, Ar-H), 7.1 (s, 6H, Ar-H), 7.49 (d, 12H, *J* 8.8, Ar-H), 7.58 (d, 12H, *J* 8.8, Ar-H), 7.65 (d, 12H, *J* 8.67, Ar-H).

3,7,8,12,13-*Pentakis*{4-[4-(4-*cyanophenyl*)*phenoxy*]*butanoyloxy*}-2-*methyl*-10,15-*dihydro*-5H-*tribenzo*[a,d,g]*cyclononene* **2a**. Yield: 55%, phase transitions (°C): Cr 163 (S_A 145) I. Elemental analysis (%): found (calc. for $C_{107}H_{85}N_5O_{15}$): C, 76.55 (76.45); H, 5.08 (5.10); N, 4.09 (4.17). δ_H ($CDCl_3$) 2.05 (s, 3H, CH_3), 2.1–2.27 (m, 10H, CH_2), 2.6–2.8 (m, 10H, CH_2COO), 3.67 (d, 3H, $ArCH_2Ar$, H_e), 3.95–4.15 (m, 10H, OCH_2CH_2), 4.7–4.85 (m, 3H, $ArCH_2Ar$, H_a), 6.9–7.73 (m, 46H, Ar-H).

3, 7, 8, 12, 13-*Pentakis*{11-[4-(4-*cyanophenyl*)*phenoxy*]*undecanoyloxy*}-2-*methyl*-10,15-*dihydro*-5H-*tribenzo*[a,d,g]*cyclononene* **2c**. Yield: 52%, phase transitions (°C): Cr 78 S_A 107 I. Elemental analysis (%): found (calc. for $C_{142}H_{155}N_5O_{15}$): C, 78.55 (78.52); H, 6.99 (7.29); N, 3.09 (3.23). δ_H ($CDCl_3$) 1.2–1.86 (m, 70H, CH_2), 2.05 (s, 3H, CH_3), 2.1–2.2 (m, 10H, CH_2), 2.6–2.8 (m, 10H, CH_2COO), 3.67 (d, 3H, $ArCH_2Ar$, H_e), 3.95–4.15 (m, 10H, OCH_2CH_2), 4.7–4.85 (m, 3H, $ArCH_2Ar$, H_a), 6.9–7.73 (m, 46H, Ar-H).

2, 3, 7, 8, 12, 13-*Hexakis*{4-[4-(5-*heptyl*-1,3,4-*thiadiazol*-2-*yl*)*phenoxy*]*butanoyloxy*}-10,15-*dihydro*-5H-*tribenzo*[a,d,g]*cyclononene* **3a**. Yield: 56%, phase transitions (°C): Cr 152 Col 182 I. Elemental analysis (%): found (calc. for $C_{135}H_{162}N_{12}O_{18}S_6$): C, 66.23 (66.64); H, 6.82 (6.71); N, 6.84 (6.91); S, 8.02 (7.91). δ_H ($CDCl_3$) 0.86 (t, 18H, *J* 6.9, CH_3), 1.24–1.8 (m, 60H, CH_2), 2.12 (m, 12H, CH_2), 2.66 (t, 12H, *J* 7, CH_2COO), 3.06 (t, 12H, *J* 7.7, $ArCH_2$), 3.69 (d, 3H, *J* 14.1, $ArCH_2Ar$, H_e), 4.0 (t, 12H, *J* 6.1, OCH_2CH_2), 4.76 (d, 3H, *J* 13.7, $ArCH_2Ar$, H_a), 6.89 (d, 12H, *J* 9, Ar-H), 7.14 (s, 6H, Ar-H), 7.79 (d, 12H, *J* 9, Ar-H). δ_C ($CDCl_3$) 170.3, 169.6, 167.9, 160.8, 140.7, 137.2, 129.4, 124.7, 123.4, 114.9, 66.6, 36.3, 31.6, 30.4, 30.2, 30.0, 29, 28.9, 24.4, 22.6, 14. Electrospray–MS: found (calc. for $C_{204}H_{264}N_{16}O_{24}S_8$): M^+ 2431.72 ± 0.22 (2431.04).

2, 3, 7, 8, 12, 13-*Hexakis*{6-[4-(5-*heptyl*-1,3,4-*thiadiazol*-2-*yl*)*phenoxy*]*hexanoyloxy*}-10,15-*dihydro*-5H-*tribenzo*[a,d,g]*cyclononene* **3c**. Yield: 59%, phase transitions (°C): Cr 151 Col 155 I. Elemental analysis (%): found (calc. for $C_{147}H_{186}N_{12}O_{18}S_6$): C, 68.13 (67.87); H, 7.38 (7.21); N, 6.42 (6.46); S, 7.21 (7.39). δ_H ($CDCl_3$) (t, 18H, *J* 6.9, CH_3), 1.2–1.8 (m, 96H, CH_2), 2.51 (t, 12H, *J* 7.05, CH_2COO), 3.08 (t, 12H, *J* 7.6, $ArCH_2$), 3.67 (d, 3H, *J* 14.2, $ArCH_2Ar$, H_e), 3.96 (t, 12H, *J* 6.3, OCH_2CH_2), 4.75 (d, 3H, *J* 13.6, $ArCH_2Ar$, H_a), 6.9 (d, 12H, *J* 8.4, Ar-H), 7.13 (s, 6H, Ar-H), 7.81 (d, 12H, *J* 8.4, Ar-H). Electrospray–MS: found (calc. for $C_{147}H_{186}N_{12}O_{18}S_6$): M^+ 2600.5 ± 1.66 (2599.23).

2,3,7,8,12,13-*Hexakis*{7-[4-(5-*heptyl*-1,3,4-*thiadiazol*-2-*yl*)*phenoxy*]*heptanoyloxy*}-10,15-*dihydro*-5H-*tribenzo*[a,d,g]*cyclononene* **3d**. Yield: 87%, mp 156 °C. Elemental analysis (%): found (calc. for $C_{153}H_{198}N_{12}O_{18}S_6$): C, 68.63 (68.43); H, 7.48 (7.43); N, 6.32 (6.26). δ_H ($CDCl_3$) 0.92 (t, 18H, CH_3, *J* 6.8), 1.2–1.8 (m, 108H), 2.56 (t, 12H, *J* 7.2, CH_2COO), 3.13 (t, 12H, *J* 7.5, $ArCH_2$), 3.72 (d, 3H, *J* 14.3 $ArCH_2Ar$, H_e), 4.01 (t, 12H, *J* 6.4, OCH_2CH_2), 4.79 (d, 3H, *J* 13.8, $ArCH_2Ar$, H_a), 6.95 (d, 12H, *J* 8.6, Ar-H), 7.18 (s, 6H, Ar-H), 7.87 (d, 12H, *J* 8.6, Ar-H); Electrospray–MS: found (calc. for $C_{153}H_{198}N_{12}O_{18}S_6$): M^+ 2683.70 ± 0.24 (2683.32).

2,3,7,8,12,13-*Hexakis*{8-[4-(5-*heptyl*-1,3,4-*thiadiazol*-2-*yl*)*phenoxy*]*octanoyloxy*}-10,15-*dihydro*-5H-*tribenzo*[a,d,g]*cyclononene* **3e**. Yield: 54%, mp 158 °C. Elemental analysis (%): found (calc. for $C_{159}H_{210}N_{12}O_{18}S_6$): C, 69.16 (68.95); H, 7.64 (7.64); N, 5.96 (6.07). δ_H ($CDCl_3$) 0.86 (t, 18H, *J* 6.95, CH_3), 1.23–1.82 (m, 120H, CH_2), 2.48 (t, 12H, *J* 7.5, CH_2COO), 3.07 (t, 12H, *J* 7.7, $ArCH_2$), 3.66 (d, 3H, *J* 14.4, $ArCH_2Ar$, H_e), 3.96 (t, 12H, *J* 6.4, OCH_2CH_2), 4.73 (d, 3H, *J* 13.4, $ArCH_2Ar$, H_a), 6.9 (d, 12H, *J* 8.65, Ar-H), 7.12 (s, 6H, Ar-H), 7.81 (d, 12H, *J* 8.85, Ar-H). δ_C ($CHCl_3$) 170.8, 169.7, 168.2, 161.3, 140.7, 137.0, 129.4, 124.6, 122.5, 120.0, 144.9, 68.0, 34.0, 31.6, 30.9, 30.1, 30.0, 29.1, 29.0, 28.9, 28.85, 25.8, 25.75, 22.6, 14.1. Electrospray–MS: found (calc. for $C_{159}H_{210}N_{12}O_{18}S_6$): M^+ 2768.67 ± 1.07 (2767.42).

2, 3, 7, 8, 12, 13-*Hexakis*{5-[4-(5-*pentadecyl*-1,3,4-*thiadiazol*-2-*yl*)*phenoxy*]*pentanoyloxy*}-10,15-*dihydro*-5H-*tribenzo*[a,d,g]*cyclononene* **3h**. Yield: 53%, phase transitions (°C): Cr_1 102 Cr_2 135 S_A 158 I. Elemental analysis (%): found (calc. for $C_{189}H_{270}N_{12}O_{18}S_6$): C, 71.23 (71.15); H, 8.8 (8.53); N, 5.3

(5.27). δ_H ($CDCl_3$) 0.86 (t, 18H, *J* 7, CH_3), 1.2–1.86 (m, 180H, CH_2), 2.57 (t, 12H, *J* 5.45, CH_2COO), 3.06 (t, 12H, *J* 7.85, $ArCH_2$), 3.67 (d, 3H, *J* 13.6, $ArCH_2Ar$, H_e), 3.98 (t, 12H, *J* 5.65, OCH_2CH_2), 4.74 (d, 3H, *J* 13.7, $ArCH_2Ar$, H_a), 6.89 (d, 12H, *J* 9, Ar-H), 7.14 (s, 6H, Ar-H), 7.80 (d, 12H, *J* 8.85, Ar-H). Electrospray–MS: found (calc. for $C_{189}H_{270}N_{12}O_{18}S_6$): M^+ 3189.17 ± 0.87 (3187.89).

2,3,7,8,12,13-*Hexakis*{6-[4-(5-*nonyl*-1,3,4-*thiadiazol*-2-*yl*)*phenoxy*]*hexanoyloxy*}-10,15-*dihydro*-5H-*tribenzo*[a,d,g]*cyclononene* **3i**. Yield: 41%, phase transitions (°C): Cr 80 Col 162 I. Elemental analysis (%): found (calc. for $C_{159}H_{210}N_{12}O_{18}S_6$): C, 69.08 (68.95); H, 7.80 (7.64); N, 5.85 (6.07). δ_H ($CDCl_3$) 0.86 (t, 18H, *J* 6.9, CH_3), 1.2–1.8 (m, 120H, CH_2), 2.51 (t, 12H, *J* 7.05, CH_2COO), 3.08 (t, 12H, *J* 6.5, Ar-CH_2), 3.67 (d, br, 3H, *J* 14.2, $ArCH_2Ar$, H_e), 3.98 (t, 12H, *J* 6.25, OCH_2CH_2), 4.75 (d, br, 3H, *J* 13.6, $ArCH_2Ar$, H_a), 6.92 (d, 12H, *J* 9, Ar-H), 7.16 (s, 6H, Ar-H), 7.83 (d, 12H, *J* 9, Ar-H).

3,7,8,12,13-*Pentakis*{6-[4-(5-*nonyl*-1,3,4-*thiadiazol*-2-*yl*)*phenoxy*]*hexanoyloxy*}-2-*methyl*-10,15-*dihydro*-5H-*tribenzo*[a,d,g]*cyclononene* **4b**. Yield: 45% phase transitions (°C): Cr 62 Col 148 I. Elemental analysis (%): found (calc. for $C_{137}H_{180}N_{10}O_{15}S_5$): C, 69.55 (69.51); H, 7.87 (7.66); N, 5.77 (5.92). δ_H ($CDCl_3$) 0.85 (t, 15H, *J* 6.4, CH_3), 1.24–1.55 (m, 60H, CH_2), 1.71–1.92 (m, 40H, CH_2), 2.06 (s, 3H, $ArCH_3$), 2.57–2.62 (m, 10H, CH_2COO), 3.06 (t, 10H, *J* 7.6, $ArCH_2$), 3.65 (d, br, 3H, *J* 13.9, $ArCH_2Ar$, H_e), 3.94–4.05 (m, 10H, CH_2O), 4.75–4.85 (m, 3H, $ArCH_2Ar$, H_a), 6.89–6.95 (m, 10H, Ar-H), 7.13–7.25 (m, 6H, Ar-H), 7.80–7.87 (m, 10H, Ar-H).

2,3,7,8,12,13-*Hexakis*{4-[4-(5-*octylpyrimidin*-2-*yl*)*phenoxy*]*butanoyloxy*}-10,15-*dihydro*-5H-*tribenzo*[a,d,g]*cyclononene* **5a**. Yield: 37%, phase transitions (°C): Cr 143 Col 170 M 177 I. Elemental analysis (%): found (calc. for $C_{153}H_{186}N_{12}O_{18}$): C, 74.39 (74.06); H, 7.74 (7.56); N, 6.54 (6.77). δ_H ($CDCl_3$) 0.86 (t, 18H, *J* 6.55, CH_3), 1.2–1.85 (m, 72H, CH_2), 2.11 (m, 12H, CH_2), 2.57 (t, 12H, *J* 7.7, $ArCH_2$), 2.67 (m, 12H, CH_2COO), 3.67 (d, 3H, *J* 13.75, $ArCH_2Ar$, H_e), 4.0 (t, 12H, *J* 6.1, OCH_2CH_2), 4.75 (d, 3H, *J* 13.55, $ArCH_2Ar$, H_a), 6.91 (d, 12H, *J* 9, Ar-H), 7.12 (s, 6H, Ar-H) 8.30 (d, 12H, *J* 9, Ar-H), 8.52 (s, 12H, Ar-H). δ_C ($CHCl_3$) 170.4, 160.8, 159.6, 156.9, 140.6, 137.1, 132.2, 129.6, 124.7, 120.5, 114.4, 66.4, 31.8, 31.2, 30.9, 30.7, 30.1, 29.9, 29.3, 29.2, 24.4, 22.6, 14.1. Electrospray–MS: found (calc. for $C_{153}H_{186}N_{12}O_{18}$): M^+ 2480.13 ± 0.43 (2479.4).

2,3,7,8,12,13-*Hexakis*{5-[4-(5-*octylpyrimidin*-2-*yl*)*phenoxy*]*pentanoyloxy*}-10,15-*dihydro*-5H-*tribenzo*[a,d,g]*cyclononene* **5b**. Yield: 45%, mp 168 °C. Elemental analysis (%): found (calc. for $C_{159}H_{198}N_{12}O_{18}$): C, 74.22 (74.44); H, 7.91 (7.78); N, 6.48 (6.55). δ_H ($CDCl_3$) 0.86 (t, 18H, *J* 6.95, CH_3), 1.15–1.95 (m, 96H, CH_2), 2.40 (t, 12H, *J* 7.1, CH_2COO), 2.57 (m, 12H, $ArCH_2$), 3.66 (d, 3H, *J* 13.9, $ArCH_2Ar$, H_e), 3.99 (t, 12H, *J* 5.5, OCH_2CH_2), 4.73 (d, 3H, *J* 13.7, $ArCH_2Ar$, H_a), 6.93 (d, 12H, *J* 8.8, Ar-H), 7.13 (s, 6H, Ar-H), 8.33 (d, 12H, *J* 8.8, Ar-H), 8.55 (s, 12H, Ar-H). Electrospray–MS; found (calc. for $C_{159}H_{198}N_{12}O_{18}$): M^+ 2564.19 ± 0.73 (2563.49).

3,7,8,12,13-*Pentakis*{5-[4-(5-*octylpyrimidin*-2-*yl*)*phenoxy*]*pentanoyloxy*}-2-*methyl*-10,15-*dihydro*-5H-*tribenzo*[a,d,g]-*cyclononene* **6**. Yield: 35%, phase transitions Cr_1 125 Cr_2 138 I. Elemental analysis (%): found (calc. for $C_{137}H_{170}N_{10}O_{15}$): C, 75.19 (74.90); H, 8.1 (7.8); N, 6.09 (6.38). δ_H ($CDCl_3$) 0.86 (m, 15H, *J* 6.5, CH_3), 2.08 (s, 3H, CH_3), 1.15–2.12 (m, 60H, CH_2), 2.5–2.7 (m, 20H, $ArCH_2$ and CH_2COO), 3.6–3.7 (m, 3H, $ArCH_2Ar$, H_e), 3.95–4.1 (m, 10H, OCH_2CH_2), 4.62–4.80 (m, 3H, $ArCH_2Ar$, H_a), 6.91–8.38 (m, br, 26H, Ar-H), 8.57 (s, 10H, Ar-H).

2,3,6,7,10,11,14,15-*Octakis*{6-[4-(4-*cyanophenyl*)*phenoxy*]*hexanoyloxy*}-5,10,15,20-*tetrahydrotetrabenzo*[a,d,g,j]*cyclododecene* **7**. Yield: 55%, phase transitions (°C): Cr_1 174 Cr_2 222 (N 220) I. Elemental analysis (%): found (calc. for $C_{180}H_{160}N_8O_{24}$): C, 76.78 (76.67); H, 5.94 (5.72); N, 3.78 (3.98). δ_H ($CDCl_3$) 1.43–1.81 (m, 48H, CH_2), 2.57 (m, br, 16H, CH_2COO), 3.7 (m, br, 8H, $ArCH_2Ar$), 3.96 (t, 16H, *J* 6.2, OCH_2CH_2), 6.6–6.9 (s, br, 8H), 6.93 (d, 16H, *J* 8.7, Ar-H), 7.46 (d, 16H, *J* 8.9, Ar-H), 7.57 (d, 16H, *J* 8.7, Ar-H), 7.63 (d, 16H, *J* 8.5, Ar-H).

2,3,6,7,10,11,14,15-*Octakis*{5-[4-(5-*nonyl*-1,3,4-*thiadiazol*-2-*yl*)*phenoxy*]*pentanoyloxy*} - 5, 10, 15, 20 - *tetrahydrotetrabenzo*[a,d,g,j]*cyclododecene* **8**. Yield: 20%, phase transitions (°C): Cr_1 142 Cr_2 204 Col 222 I. Elemental analysis (%): found (calc. for $C_{204}H_{264}N_{16}O_{24}S_8$): C, 68.22 (68.43); H, 7.52 (7.43); N, 6.14 (6.26). δ_H ($CDCl_3$) 0.86 (t, 24H, *J* 7, CH_3), 1.2–1.9 (m, 160H, CH_2), 2.6 (m, 16H, CH_2COO), 3.08 (t, 16H, *J* 7.5 $ArCH_2$), 3.7 (m, br, 8H, $ArCH_2Ar$), 3.99 (m, 16H, O-CH_2-CH_2), 6.6–6.9 (m, br, 8H, Ar-H), 6.89 (d, 16H, *J* 8.2, Ar-H), 7.81 (d, 16H, *J* 8.2, Ar-H). Electrospray–MS: found (calc. for $C_{204}H_{264}N_{16}O_{24}S_8$): M^+ 3579.91 ± 0.86. (3580.91).

2,3,6,7,10,11,14,15-*Octakis*{5-[4-(5-*octylpyrimidin*-2-*yl*)-*phenoxy*]*pentanoyloxy*} - 5, 10, 15, 20 - *tetrahydrotetrabenzo*[a,d,g,j]*cyclododecene* **9**. Yield: 10%, mp 241 °C. δ_H ($CDCl_3$) 0.85 (t, 24H, CH_3), 1.15–1.95 (m, 128H, CH_2), 2.5–2.57 (m, 32H, $ArCH_2$ and CH_2COO), 3.7 (m, br, 8H, $ArCH_2Ar$), 3.98 (t, 16H, OCH_2CH_2), 6.6–6.9 (m, br, 8H, Ar-H), 6.92 (d, 16H, *J* 8.7, Ar-H), 8.31 (d, 16H, *J* 8.9, Ar-H), 8.53 (s, 16H, Ar-H).

This work was supported by the BMBF and the Fonds der Chemischen Industrie.

References

1 B. Bahadur, *Liquid Crystals Application and Uses*, World Scientific, Singapore, 1990, Vol. 1–3.
2 D. M. Walba, M. B. Ros, T. Sierra, J. A. Rego, N. A. Clark, R. Shao, M. D. Wand, R. T. Vohra, K. E. Arnett and S. P. Velsco, *Ferroelectrics*, 1991, **121**, 147; K. Schmitt, R.-P. Herr, M. Schadt, J. Fünfschilling, R. Buchecker, X. H. Chen and C. Benecker, *Liq. Cryst*., 1993, **14**, 1735.
3 F. Closs, K. Siemensmeyer, Th. Frey and D. Funhof, *Liq. Cryst*., 1993, **14**, 629.
4 S. Chandrasekhar, *Liq. Cryst*., 1993, **14**, 3.
5 S. Chandrasekhar, *Mol. Cryst. Liq. Cryst*., 1994, **243**, 1.
6 K. Borisch, S. Diele, P. Göring, H. Müller and C. Tschierske, *Liq. Cryst*., 1995, **18**, 175.
7 H.-T. Nguyen, C. Destrade and J. Malthete, *Adv. Mater*., 1997, **9**, 375.
8 I. D. Fletcher and G. R. Luckhurst, *Liq. Cryst*., 1995, **18**, 175.
9 W. Kreuder, H. Ringsdorf, O. Herrmann-Schönherr and J. H. Wendorff, *Angew. Chem*., 1987, **99**, 1300.
10 H. Budig, S. Diele, P. Göring, R. Paschke, C. Sauer and C. Tschierske, *J. Chem. Soc., Chem. Commun*., 1994, 2359.
11 H. Budig, S. Diele, P. Göring, R. Paschke, C. Sauer and C. Tschierske, *J. Chem. Soc., Perkin Trans. 2*, 1995, 767.
12 J. Malthete and A. Collet, *J. Am. Chem. Soc*., 1987, **109**, 7544.
13 H. Zimmermann, R. Poupko, Z. Luz and J. Billard, *Z. Naturforsch. Teil A*, 1985, **40**, 149.
14 L. Lei, *Mol. Cryst. Liq. Cryst*., 1987, **146**, 41.
15 H. Zimmermann, R. Poupko, Z. Luz and J. Billard, *Z. Naturforsch. Teil A*, 1986, **41**, 1137.
16 C. Tschierske and H. Zaschke, *J. Prakt. Chem*., 1989, **331**, 365.
17 A. S. Lindsey, *J. Chem. Soc*., 1965, 1685.
18 V. Percec, C. G. Cho and C. Pugh, *J. Mater. Chem*., 1991, **1**, 217.
19 G. W. Gray, K. J. Harrison and J. A. Nash, *Pramana*, 1975, **1**, 381.
20 A. Collet, *Tetrahedron*, 1987, **43**, 5725; J. A. Hyatt, E. N. Duesler, D. Y. Curtin and I. C. Paul, *J. Org. Chem*., 1980, **45**, 5074; A. Collet, J. Gabard, J. Jacques, M. Cesario, J. Guilhem and C. Pscard, *J. Chem. Soc., Perkin Trans*., 1981, 1630.
21 P. Barois, J. Pommier and J. Prost, in *Solitons in Liquid Crystals*, ed. L. Lam and J. Prost, Springer, Heidelberg, 1991, p. 191.

22 B. J. Ostrovskii, *Liq. Cryst*., 1993, **14**, 131.
23 F. Hardouin, A. M. Levelut, M. F. Achard and Sigaud, *J. Chim. Phys*., 1983, **80**, 53.
24 F. Hardouin, A. M. Levelut and G. Sigaud, *J. Phys. Fr*., 1981, **42**, 71.
25 W. Weissflog, A. Wiegeleben, S. Diele and D. Demus, *Liq. Cryst*., 1984, **19**, 983.
26 J. Watanabe, Y. Nakata and K. Simizu, *J. Phys. II*, 1994, **4**, 581.
27 P. Davidson, P. Keller and A. M. Levelut, *J. Phys*., 1985, **46**, 939.
28 B. W. Endres, M. Ebert, J. H. Wendorff, B. Reck and H. Ringsdorf, *Liq. Cryst*., 1990, **7**, 217.
29 T. A. Lobko and B. I. Ostrovskii, *Mol. Mater*., 1992, **1**, 99.
30 H. T. Nguyen, G. Sigaud, M. F. Achard, F. Hardouin, R. J. Twieg and K. Betterton, *Liq. Cryst*., 1991, **10**, 389.
31 R. W. Date, G. R. Luckhurst, M. Shuman and J. M. Seddon, *J. Phys*., 1995, **42**, 587.
32 F. Hardouin, M. F. Achard, J.-I. Jin and Y.-K. Yun, *J. Phys. II*, 1995, **5**, 927.
33 V. Faye, F. Babeau, F. Placin, H. T. Nguyen, P. Barios, V. Laux and N. Isaert, *Liq. Cryst*., 1996, **21**, 485.
34 T. Niori, T. Sekine, J. Watanabe, T. Furukawa and H. Takazoe, *J. Mater. Chem*., 1996, **6**, 1231.
35 C. Tschierske, H. Zaschke, H. Kresse, A. Mädicke and D. Demus, *Mol. Cryst. Liq. Cryst*., 1990, **191**, 223.
36 H. Zaschke and R. Stolle, *Z. Chem*., 1975, **15**, 441.
37 *Organicum*, Deutscher Verlag der Wissenschaften, Berlin 1993, pp. 577 and 591.
38 A. M. Levelut and K. Moriya, *Liq. Cryst*., 1996, **20**, 119.
39 G. H. Mehl and J. W. Goodby, *Chem. Ber*., 1996, **129**, 521.
40 P. Göring, G. Pelzl, S. Diele, P. Delavier, K. Siemensmeyer and K. H. Etzbach, *Liq. Cryst*., 1995, **19**, 629.

Paper 7/02034A; *Received* 24*th March*, 1997